Journal of Alloys and Compounds 551 (2013) 286–292

Contents lists available at SciVerse ScienceDirect

Journal of Alloys and Compounds

journal homepage: www.elsevier.com/locate/jalcom

One-step hydrothermal synthesis of C, W-codoped mesoporous TiO_2 with enhanced visible light photocatalytic activity

Qi Xiao *, Lan Gao

School of Resources Processing and Bioengineering, Central South University, Changsha 410083, China

ARTICLE INFO

Article history:
Received 15 August 2012
Received in revised form 28 September 2012
Accepted 10 October 2012
Available online 22 October 2012

Keywords:
C, W-codoped mesoporous TiO_2
One-step hydrothermal method
Photocatalytic activity
Visible light

ABSTRACT

C, W-codoped mesoporous TiO_2 is prepared by one-step hydrothermal method and characterized by X-ray diffraction (XRD), Raman spectra, transmission electron microscopy (TEM), high-resolution transmission electron microscopy (HRTEM), X-ray photoelectron spectra (XPS), Brunauer–Emmett–Teller method (BET), and UV–vis diffuse reflectance spectroscopy (DRS). The C, W-codoped TiO_2 exhibited the highest photocatalytic activity under visible light irradiation compared with undoped TiO_2, C-doped TiO_2 and W-doped TiO_2 because the co-operation of C and W not only led to the much narrowing of the band gap, but also promoted the separation of the photo-generated electrons and holes.

1. Introduction

Mesoporous TiO_2 is attracting increasing attentions for the application as highly efficient photocatalysts and energy-converters due to high specific surface area [1]. However, more widespread applications of mesoporous TiO_2 as photocatalysts are encumbered by its wide band gap (3.2 eV for anatase). Further, photoexcited electron–hole pairs tend to recombine relatively easily in TiO_2. Therefore, it is highly desirable to extend the optical absorption of TiO_2-based mesoporous materials to the visible-light region with a low photogenerated electron–hole recombination rate.

In general, doping is one of the most effective approaches to extend the absorption edge from ultraviolet to the visible light range. Thus, a large number of investigations focusing on doping of TiO_2 with have been reported during the past decade and demonstrated obvious visible-light activity. Many studies have revealed that doping TiO_2 with transition metal [2,3] or nonmetal elements [4–7] can shift its optical response to the visible light region, therefore increasing visible light photocatalytic activity. However, many studies have demonstrated that the monodoping (transition metal [8,9] or nonmetal [10,11]) will generate recombination centers of photogenerated electron–hole inside the TiO_2, resulting in the reduction of charge carrier quantity and photocatalytic activity [8–11]. Recently, both theoretical calculations [12–18] and experimental results [19–23] indicated that the passivated codoped TiO_2 with both nonmetal anions and metal cations can reduce the recombination centers because of the neutralization of positive and negative charges inside TiO_2, which can effectively improve the charge carriers' migration efficiency and then enhance the photocatalytic activity. These results suggest that mesoporous TiO_2 passivated codoped with nonmetal and transition metal elements can have promising visible light photocatalytic properties.

Although numerous reports on mesoporous TiO_2 doped with metal or nonmetals have been presented [24–31], the preparation of C, W-codoped mesoporous TiO_2 has never been reported. According to the previous theoretical calculation results [14], the present work tries to experimentally fabricate the C, W-codoped mesoporous TiO_2 by using a simple one-step hydrothermal method and to evaluate its visible light photocatalytic properties. In the present study, we synthesize the C, W-codoped mesoporous TiO_2 based on the contributions of Dong et al. [31]. C, W-codoped mesoporous TiO_2 with anatase phase are synthesized by simple one-step hydrothermal method with low-cost inorganic $Ti(SO_4)_2$, glucose, and Na_2WO_4 as precursors. The resulting C, W-codoped mesoporous TiO_2 exhibit enhanced photocatalytic activity compared to C-doped TiO_2 and W-doped TiO_2. To the best of our knowledge, this method is the first report on a one-step green synthetic route for C, W-codoped mesoporous TiO_2 with efficient visible light photocatalytic activity.

2. Experimental

2.1. Preparation of samples

C, W-codoped TiO_2 is synthesized by one-step hydrothermal method. In a typical synthesis, 4.8004 g Ti $(SO_4)_2$, 0.0396 g glucose and appropriate amount of Na_2WO_4 are mixed in 100 ml of distilled water to form an aqueous solution. The

---

* Corresponding author. Tel.: +86 731 88830543; fax: +86 731 88879815.
E-mail address: xiaoqi88@mail.csu.edu.cn (Q. Xiao).

0925-8388/$ - see front matter © 2012 Elsevier B.V. All rights reserved.
http://dx.doi.org/10.1016/j.jallcom.2012.10.040

molar ratio of W to Ti is controlled at 10%. The as-prepared samples are labeled as C, W-codoped TiO_2. After stirring for 0.5 h, the solution is poured into a Teflon-lined stainless autoclave with 200 ml capacity. The autoclave is sealed and heated, and then kept at a certain temperature in a range from 150 °C for 12 h. The resulting product is separated by centrifugation, and washed with distilled water and alcohol for several times, respectively, and finally, dried at 80 °C for 6 h. For comparison purposes, the samples of pure TiO_2, C-doped TiO_2, and 10% W-doped TiO_2 are also prepared by similar procedures, respectively. The as-prepared samples are labeled as undoped TiO_2, C-doped TiO_2, and W-doped TiO_2, respectively.

2.2. Characterization methods

The X-ray diffraction (XRD) patterns of the synthesized samples are obtained by a Brucker D8-advance X-ray powder diffractometer (XRD) with Cu Kα radiation (λ = 0.15418 nm). Raman spectrum analysis is conducted on a Labram HR800 Laser Raman Spectroscopy made by Jobin Yvon, France, using the 632.8 nm He–Ne ion laser as an excitation source. The laser power on the sample is 10 mW. Transmission electron microscopy (TEM) images are obtained using a JEM-2100F transmission electron microscope. X-ray photoelectron spectra (XPS) measurements are performed in a VG Scientific ESCALAB Mark II spectrometer equipped with two ultra-high vacuum (UHV) chambers using Al Kα radiation (1486.6 eV) to investigate the surface properties. The binding energy of the XPS spectra is calibrated with the reference to the C 1s peak (284.8 eV) arising from adventitious carbon. Ar^+ sputtering is applied to clean the surface of the samples. Nitrogen adsorption and desorption isotherms are collected at 77 K on a Micromeritic ASAP 2010 instrument. The specific surface areas are calculated using the Brunnauer–Emmett–Teller (BET) equation and the pore size distributions are calculated by applying the Barrett–Joyner–Halenda (BJH) method using the desorption branch of the isotherms. The UV–vis absorption spectra are measured under the diffuse reflection mode using the integrating sphere attached to a Shimadzu 2450 UV–vis spectrometer. The powders are pressed to form a pellet and $BaSO_4$ is used as a reference.

2.3. Photocatalytic activity measurements

The photocatalytic activities of the samples are evaluated by the degradation of terephthalic acid (TA) in an aqueous solution under visible light irradiation. The analysis of $^{\cdot}$OH radical's formation on the sample surface under visible light irradiation is performed by fluorescence technique using terephthalic acid, which readily reacted with $^{\cdot}$OH radicals to produce highly fluorescent product, 2-hydroxyterephthalic acid [32]. The intensity of the peak attributed to 2-hydroxyterephthalic acid is known to be proportional to the amount of $^{\cdot}$OH radicals formed [32]. The selected concentration of terephthalic acid solution is 5×10^{-4} M in a diluted NaOH aqueous solution with a concentration of 2×10^{-3} M. It has been proved that at these experimental conditions (low concentration of terephthalic acid, less than 10^{-3} M, room temperature), the hydroxylation reaction of terephthalic acid proceeds mainly by $^{\cdot}$OH radicals [32]. Five hundred milligrams of the prepared samples is added to 100 mL of the 5×10^{-4} M terephthalic acid solution in 2×10^{-3} M NaOH under ultrasonic vibration for 10 min. Prior to light irradiation, the reactor is left in the dark for at least 30 min until an adsorption–desorption equilibrium is finally established. A 100 W tungsten lamp fixed at a distance of 150 mm above the surface solution is used as visible light source, and a UV cut-off filter is used to completely remove any radiation below 420 nm to ensure illumination by visible light source only. The average irradiation intensity of 100 W tungsten lamp was about 0.7 mW cm^{-2}. The radiant flux was measured with a power meter from Institute of Electric Light Source (Beijing). Sampling is performed in every 15 min. Solution after filtration through 0.45 μm membrane filter is analyzed on a Hitachi F-4500 fluorescence spectrophotometer. The product of terephthalic acid hydroxylation, 2-hydroxyterephthalic acid, gave a peak at the wavelength of about 425 nm by the excitation with the wavelength of 315 nm.

3. Results and discussion

3.1. XRD, Raman spectroscopy and TEM analysis

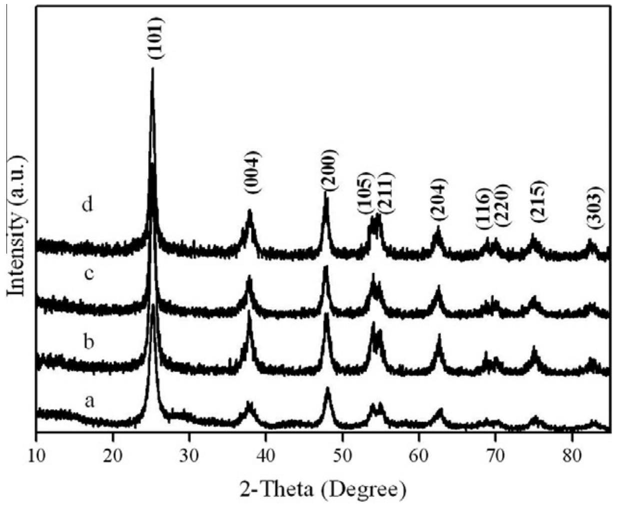

Fig. 1. The XRD patterns of the as-prepared samples. (a) undoped TiO_2; (b) C-doped TiO_2; (c) C, W-codoped TiO_2; (d) W-doped TiO_2.

Fig. 1 shows the XRD patterns of the as-prepared samples. The diffraction peaks of each sample can be indexed to anatase phase with lattice parameters $a = b = 0.37852$ nm, $c = 0.95139$ nm, and space group $I4_1/amd$ (141) (JCPDS No. 21-1272). No traces of impurity peaks other than TiO_2 are observed. In the case of XRD of C-doped or C, W-codoped TiO_2, no characteristic peak from carbon was detected in XRD, indicating that C ion has been substituted into the crystal lattice sites of the titania or amorphous carbon exists over the titania surface. It is worth noting that no WO_3 phase can be observed in all the XRD patterns of C, W-doped TiO_2 and W-doped TiO_2. On the basis of this, it can be inferred that either the W ion has been substituted into the crystal lattice sites of the titania or the tungsten oxide species exist as a highly dispersed polymeric form over the titania surface, which could not be detected by XRD. The averaged crystallite sizes D is determined according to the Scherrer equation $D = k\lambda/\beta\cos\theta$ [33], where k is a constant (shape factor, about 0.9), λ is the X-ray wavelength (0.15418 nm), β is the full width at half maximum (FWHM) of the diffraction line, and θ is the diffraction angle. The values of β and θ of anatase are taken from anatase (1 0 1) diffraction line. The calculated averaged crystallite sizes of the as-prepared samples are shown in Table 1. It is found that the crystallite sizes of the as-prepared samples are about 12–14 nm.

Fig. 2 shows the Raman spectra of the as-prepared samples. It is found that the typical Raman peaks of anatase are detected in each sample, which reports that the characteristic Raman peaks of anatase locate at 144 cm^{-1} (E_g), 399 cm^{-1} (B_{1g}), 515 cm^{-1} (A_{1g}) and 639 cm^{-1} (E_g) [34]. The characteristic Raman peaks for WO_3 were observed by Daniel et al. at 807, 715, 324, 293, and 270 cm^{-1} [35]. Interestingly, the Raman spectra in the present work did not show any trace of WO_3, implying that WO_3 does not exist as a separate crystalline oxide phase. There is also a significant decrease in the intensity of the Raman peaks with the increase of the W doping concentration. On the basis of these Raman spectroscopic observations, it can be inferred that the W ion is doped in the titania lattice, which is in agreement with the XRD results. In addition, the main peak intensity (146 cm^{-1}) of C-doped TiO_2 with no change in the peak position decreases compared with that of undoped TiO_2, which can be inferred that carbon is doped in the TiO_2 lattice [36].

The structure and morphology of the sample are further examined by transmission electron microscopy (TEM) and high-resolution transmission electron microscopy (HRTEM). The TEM and corresponding HRTEM images of the C, W-codoped TiO_2 sample are presented in Fig. 3. It can be seen that the primary crystallite size is about 13 ± 1 nm (Fig. 3a), which is in agreement with the value of the crystallite size determined by XRD (as shown in Table 1). Fig. 3b shows clear lattice fringes of primary crystallite (0.35 nm corresponding to) of the same sample, The HRTEM image (Fig. 3b) shows that the fringe spacing is 0.35 nm, which corresponds to the (1 0 1) crystallographic plane of anatase, and the HRTEM picture and its corresponding FFT (inset in Fig. 3b) further demonstrates that the particle is single crystalline in nature, and there are no indications of secondary phases or impurities visible in the HRTEM pictures, suggesting that all dopant atoms are homogeneously incorporated into the TiO_2 nanocrystallines.